Contactless Respiration Monitoring During Sleep with a pair of Wi-Fi devices

Hongyang Zhuo, Qinghua Zhong*
School of Physics and Telecommunication Engineering
South China Normal University
Guangzhou, China
*Corresponding Author: zhongqinghua@m.scnu.edu.cn

Xin Zhuo
Department of Nursing
The Second Affiliated Hospital of Shandong First Medical University
Taian, China

2022 IEEE MTT-S International Microwave Biomedical Conference (IMBioC) | 978-1-6654-2340-3/22/$31.00 ©2022 IEEE | DOI: 10.1109/IMBIOC52515.2022.9790212

***Abstract*—It is essential to detect human breathing signals during sleep because it can help us discover some potential disease risks in time. In recent years, contactless respiration detection based on WiFi signals has aroused extensive research interest. The paper adopts a pair of off-the-shelf WiFi devices and exploits the fine-grained channel state information (CSI) to track the respiration rate during sleep. We present a novel method to combine the amplitude and phase of the CSI ratio to address the "blind spots" issue. Our system utilizes two complementary antenna pairs to perform respiration monitoring based on the Fresnel zone model. Extensive experiment results demonstrate that our system can achieve contactless and sustainable detection of a person's respiration in different sleeping positions.**

Keywords—Wi-Fi, channel state information, sleep monitoring, respiration

I. Introduction

In recent years, contactless respiration detection based on radio-frequency signals has developed significantly. For example, continuous frequency modulation wave (FMCW) radars and Doppler radars can detect the chest wall movement caused by respiration to measure breathing rate. In addition, Universal Software Radio Peripherals and ultra-wideband radars can also be used to detect human breathing. However, due to the high cost of the specially designed hardware, they are not suitable for home use. Benefiting from the convenience of wear-free devices and reusing the ubiquitous WiFi infrastructure in cities, WiFi-based schemes have attracted a lot of attention.

Previous WiFi-based monitoring works (e.g. [1], [2], [3]) used the amplitude of the channel state information (CSI) to extract the personal respiratory data in different sleeping positions. Compared with the amplitude information, the phase information is more robust. However, the phase information extracted from a single antenna carries random noise from the transceiver equipment, the phase information cannot be leveraged directly. Wang et al. [4] proposed and verified the phase difference method to eliminate random noise in the phase. Nevertheless, no matter the CSI amplitude information or the CSI phase information is used alone, it is difficult to detect the slight movement caused by respiration when a person is in a certain special position [5], which is called the "blind-spot" issue [6]. Recently, Zeng et al. [7] proposed a method to combine the amplitude and phase of the CSI ratio by selecting the projection coordinate axis in the entire complex plane based on periodicity, which removed the "blind spots".

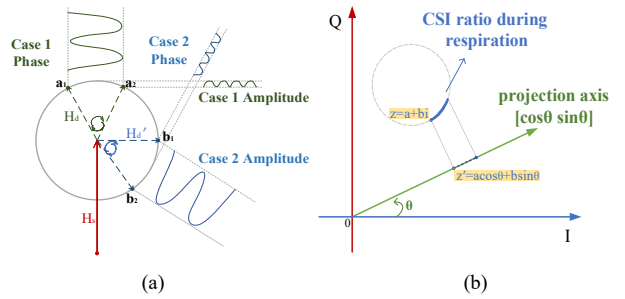

Fig. 1. The CSI or CSI ratio trajectory shows in the complex plane during respiration. (a) The amplitude and phase of the CSI in different cases. (b) The CSI ratio trajectory and its rotation projection axis.

However, the previous scheme [7] has a flaw in selecting the fixed projection coordinate axis to generate a respiration pattern, which only exploits the periodic feature. Some bad respiration patterns can be obtained even in the case of desirable CSI ratio variation, which constraints greatly limit the real-life application of the existing approaches.

To solve the above problem, we propose to combine the periodicity and variance features to select the projection coordinate axis, which improves the robustness of respiration monitoring. Furthermore, we exploit the complementarity of antenna pairs to track the respiration rate based on the Fresnel zone model [5]. The mean accuracy of 97.25% can be obtained for single-person respiration rate estimation in different sleeping positions under the non-line-of-sight scenario.

II. Theoretical Basis

Radio-frequency signals propagate along multiple paths in the room where WiFi devices are placed. The propagation paths of radio-frequency signals can be divided into static paths and dynamic paths. The static path signals caused by the reflection and diffraction of static objects in the environment are barely unchanged. While people or objects move in the environment, they change the dynamic propagation paths continuously. Every signal received from the receiver antenna is the superposition of all static path signals (H_s) and dynamic path signals (H_d). The WiFi CSI describes the path change experienced by the received signal. Thus, we can analyze the CSI to infer and perceive the chest wall movement caused by human respiration. Due to the movement of the chest wall having very little change during respiration, the CSI trajectory is a small circular arc in Fig. 1(a).

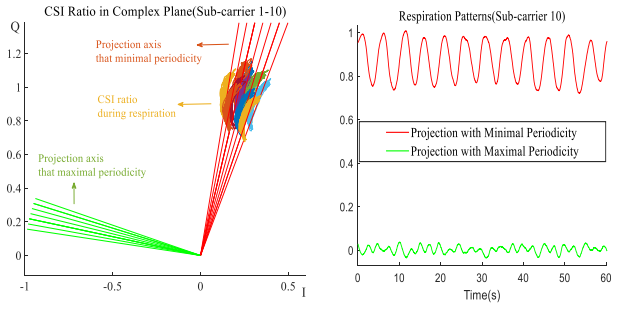

(a) (b)

Fig. 2. The CSI ratio trajectories and their projection signals during the continuous 60-second respiration. (a) The CSI ratio trajectories of the first ten subcarriers and their corresponding maximal periodic projection axis and minimal periodic projection axis. (b) Projection signals of subcarrier number 10 in different projection axis.

As shown in Fig. 1(a), whether it is amplitude or phase of CSI used alone, there is no guarantee that an excellent respiratory waveform can be obtained under all conditions. For this problem, we use the method of selecting the projection coordinate axis in the entire complex plane rather than directly using the amplitude and phase of CSI, which provides more and better choices. Fig. 1(b) shows how a point z is projected on an axis [cosθ sinθ] to get a new point z′, where θ is the angle of projection axis. Specifically, we adopt the short-term breathing-to-noise ratio (BNR) to measure the periodicity of the respiration signal, which is calculated by dividing the frequency band energy of the projected signal in the human breathing range (10 bpm to 37 bpm) by the overall energy. In the range where the parameter θ varies from 0 to 2π, the projection coordinate axis with the maximal BNR value is selected for projection to obtain a respiration signal.

III. Breath Detection Algorithm

A. Data preprocessing

We divide the complex CSI data from the two transmitting antennas to obtain the CSI ratio. The Savitzky-Golay filter is adopted to smooth the CSI ratio data of each sub-carrier and the CSI ratio trajectory during respiration is still a circular arc in the complex plane, as illustrated in Fig. 1(b).

B. Breathing mode selection

The selected parameter θ based on periodicity has a deviation of about 90° in some cases. The CSI ratio trajectory generated during the continuous 60-second respiration is shown in Fig. 2(a). The green lines indicate the projection coordinate axis with the maximal periodicity selected for each sub-carrier, i.e., the BNR value is the largest. It can be seen that the most suitable projection coordinate axis should be near the red lines. Furthermore, taking the subcarrier number 10 as an example, we project its CSI ratio trajectory on the maximal periodic coordinate axis and the minimal periodic coordinate axis. Fig. 2(b) shows the two projection respiration patterns, respectively. Comparing the two respiration patterns, we can see that the red waveform has greater amplitude and more obvious periodicity. The frequency of the red waveform is also closest to the actual breathing rate, but the frequency of the green waveform selected based on the maximal periodicity is twice the ground truth.

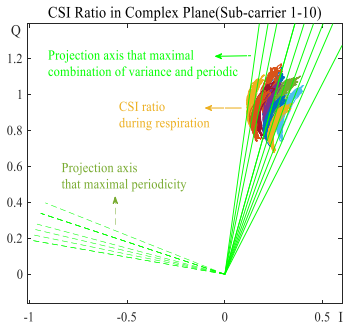

Fig. 3. The CSI ratio trajectories of the first ten subcarriers and their projection axis that selected by different algorithms during the continuous 60-second respiration.

Why is the optimal projection axis considered to be the projection axis with the minimal periodic? Through the analysis of the time and frequency domain of the respiration patterns, it is concluded that the red projection signal has a DC component, and the significant discontinuity is produced after zero padding. There are apparent frequencies around 0 Hz in the frequency domain. In this case, the overall energy value of the signal is one order of magnitude higher than the energy value of the bandpass signal. As for the green projection signal, its projection area is near the origin and has almost no DC component. Therefore, the BNR value of the red signal is far less than the BNR value of the green signal and the error projection axis has been chosen. To address this issue, we apply the Hampel filter to remove the DC component of all signals after projection.

Even after the above processing, the BNR value of the green signal is slightly larger than that of the red signal in Fig. 2(b), it is a spectrum leakage problem [8]. Compared with the red projection signal, the green projection signal has more cycles in the same unit of time. Moreover, the green projection signal is less affected by zero-padding due to its small amplitude. In general, this green signal has stronger signal integrity than others in a short time, so we introduce a new feature to address this issue. Considering that the amplitude of the two signals after projection is quite different, we combine the variance and periodicity of respiration patterns to select the projection coordinate axis. The compare result is shown in Fig. 3. As can be seen, the reselected projection coordinate axis is more accurate. No matter what the situation is, an excellent projection coordinate axis can be selected. Since people stay still most of the time during sleep, we use the first 12-second respiration data to select the projection coordinate axis to estimate the respiration rate within three minutes, which is acceptable for a real-time respiration monitoring system.

C. Respiration rate estimation

1) SG filtering. We apply the Savitzky-Golay filter to remove the noise and smooth the projection signal.

2) False peak removal. In addition to false peaks caused by the instability of the WiFi channel, the selected projection coordinate axis is not directly aligned with the CSI ratio trajectory due to insufficient step size accuracy, which may also cause false peaks. Just in case, we use the method of false peak detection [2] to remove it.

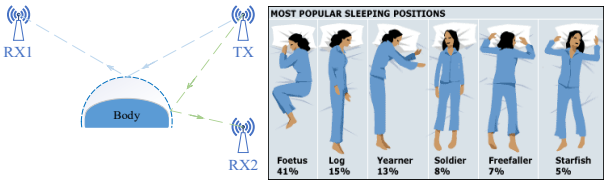

(a) (b)

Fig. 4. Experimental setup. (a) The relative position of the antennas and the person. (b) The most popular sleeping positions.

3) Peak-to-peak detection. After capturing all true peaks from each sub-carrier, we combine the peak-to-peak time intervals to calculate the breathing rate of each sub-carrier. According to the variance, we use a weighted mean of the breathing rates from multiple subcarriers to obtain a more accurate breathing rate estimation.

IV. Experiment Setup and Experiment Results

The WiFi transmitting device used in our experiment is a wireless router (i.e., TP-Link TL-WDR5610), the carrier center frequency is set at 5.785 GHz, and the bandwidth is 20 MHz. The receiving device is a micro host that runs Ubuntu 14.04 LTS and is equipped with an Intel 5300 network card. The sampling rate is set to 100 Hz. The layout of antennas is shown in Fig. 4(a). We utilize four antennas (i.e., the two antennas at the WiFi transmitter TX, the receiver antenna RX1, the receiver antenna RX2). The distance between TX and RX1 is 180 cm, and the distance between TX and RX2 is 100 cm. The receiver antenna RX2 is set to be slightly higher than the height of the bed surface. All antennas are common omnidirectional antennas and are placed parallel to the ground.

We gathered 11 volunteers (nine male and two female students) to perform breathing detection in the conference room for nearly three months for different sleeping positions. Specifically, as shown in Fig. 4(b), we ask each volunteer to adopt the most popular sleeping positions [9] in turn. The same orientations are adopted as the sleeping position in Fig. 4(b). We adopt the frequency of the metronome as the ground truth, and each volunteer follows the three frequencies of the metronome (i.e., 0.2 Hz, 0.25 Hz, 0.3 Hz) to breathe, and the test is performed for three minutes each time.

We set different weights for periodicity and variance to compare the accuracy of respiration detection and evaluated the overall performance in different sleeping positions. As shown in Fig. 5(a), the performance of respiration detection decreases significantly when the periodicity is assigned a weight over 0.8. Extensive experimental results show that our respiratory monitoring method is more robust than previous schemes. Furthermore, we set the periodicity and variance weights to 0.6 and 0.4 in Fig. 5(b), respectively. The results show the complementarity of the TX-RX1 and TX-RX2 pairs for detection. Overall, our system achieved the high performance with the mean absolute error of less than 0.14 bpm and the mean accuracy of 97.25% across the six sleep positions.

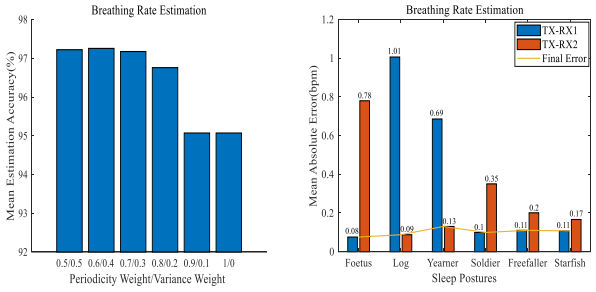

(a) (b)

Fig. 5. Experiment results. (a) Mean accuracy of the estimated breathing rate of all sleeping positions under different weights. (b) Mean absolute error of breathing rate estimation versus the sleeping positions.

V. Conclusion

In this paper, we present a novel method to combine the CSI ratio's amplitude and phase to address the "blind spots" issue. We establish the complementary antenna pairs based on the Fresnel zone model to perform respiration detection on all the most popular sleeping positions. The preliminary results show that our method has the better robustness of respiration monitoring, which will be helpful for future work.

Acknowledgment

The authors are indebted to all volunteers for their assistance in our experiments.

References

[1] X. Liu, J. Cao, S. Tang, J. Wen, and P. Guo, "Contactless Respiration Monitoring Via Off-the-Shelf WiFi Devices," IEEE Trans. Mob. Comput., vol. 15, no. 10, pp. 2466–2479, Oct. 2016.

[2] J. Liu, Y. Chen, Y. Wang, X. Chen, J. Cheng, and J. Yang, "Monitoring Vital Signs and Postures During Sleep Using WiFi Signals," IEEE Internet Things J., vol. 5, no. 3, pp. 2071–2084, Jun. 2018.

[3] Y. Gu, X. Zhang, Z. Liu, and F. Ren, "WiFi-Based Real-Time Breathing and Heart Rate Monitoring during Sleep," in IEEE Glob. Commun. Conf., Waikoloa, HI, USA, Dec. 2019, pp. 1–6.

[4] X. Wang, C. Yang, and S. Mao, "PhaseBeat: Exploiting CSI Phase Data for Vital Sign Monitoring with Commodity WiFi Devices," in IEEE Int. Conf. Distrib. Comput. Syst., Atlanta, GA, USA, Jun. 2017, pp. 1230–1239.

[5] H. Wang et al., "Human respiration detection with commodity wifi devices: do user location and body orientation matter?," in Proc. ACM Int. Jt. Conf. Pervasive Ubiquitous Comput., Heidelberg Germany, Sep. 2016, pp. 25–36.

[6] Y. Zeng, D. Wu, R. Gao, T. Gu, and D. Zhang, "FullBreathe: Full Human Respiration Detection Exploiting Complementarity of CSI Phase and Amplitude of WiFi Signals," Proc. ACM Interact. Mob. Wearable Ubiquitous Technol., vol. 2, no. 3, pp. 1–19, Sep. 2018.

[7] Y. Zeng, D. Wu, J. Xiong, E. Yi, R. Gao, and D. Zhang, "FarSense: Pushing the Range Limit of WiFi-based Respiration Sensing with CSI Ratio of Two Antennas," Proc. ACM Interact. Mob. Wearable Ubiquitous Technol., vol. 3, no. 3, pp. 1–26, Sep. 2019.

[8] Feng Han, Yanxia Wang, and Meixian Hao, "Leakage analysis and Its application in calculating a sinusoidal parameters," in Int. Conf. Comput. Des. Appl., Qinhuangdao, China, Jun. 2010, pp. V2-6-V2-9.

[9] "BBC NEWS | Health | Sleep position gives personality clue." [Online]. Available: http://news.bbc.co.uk/2/hi/health/3112170.stm.